Performance of digital algorithms for n/γ pulse shape discrimination using a liquid scintillation detector

P. J. Sellin*, G. Jaffar and S. D. Jastaniah

Department of Physics, University of Surrey, Guildford GU2 7XH, UK.

Abstract--We have investigated the use of digital data acquisition techniques to analyze the performance of pulse shape discrimination from a liquid scintillation detector in mixed neutron/gamma radiation fields. Three digital pulse shape discrimination methods were explored, applied to pulses digitized from a liquid scintillator using a high-speed waveform digitizer. The various features of these digital discrimination techniques are discussed and quality of the resulting n/γ pulse shape discrimination is compared. The digital approach is useful with regard to developing a compact neutron monitor that is capable of fast neutron spectroscopy in the presence of strong mixed n/γ radiation fields

I. INTRODUCTION

Liquid scintillators continue to be the material of choice for n/γ discrimination due to their superior pulse shape discrimination(PSD) properties [1]. The use of PSD in liquid scintillators relies on the presence of long lifetime components of the scintillation light produced by high LET events such as proton recoils due to neutron scatter events. In the past, this phenomenon has been extensively studied using analogue pulse shape discrimination techniques including the two widely used methods of rise time, characterized by a simple measurement of the time interval between 10% and 90% of the amplitude of the integrated pulse amplitude [2] and the second method is the charge comparison that implies the determination of the relative weight of the amount of light emitted respectively in the fast and slow components of the light pulse [3]. The implementation of the method generally relies upon the integration of the pulse over two different time intervals.

The availability of high-speed waveform digitizers with sampling times of the order of 1 ns has made possible the complete digitization of pulses from liquid scintillators on an event-by-event basis. The application of various digital PSD algorithms can potentially achieve enhanced n/γ discrimination compared to previous analogue techniques. We have reported [4] the use of a digital pulse rise-time algorithm to achieve good n/γ discrimination in boron-loaded liquid scintillator. Most recently, other authors have reported the use of direct waveform digitization of PMT pulses to investigate digital PSD performance both in stilbene [5] and in liquid scintillators [6]. These studies have concentrated on more complex pulse shape analysis, typically using linear regression techniques to fit a calculated response function to each pulse. Such techniques are highly computationally intensive and poorly suited for real-time processing in potential field instruments. In this paper we have concentrated on the use of computationally simple PSD algorithms that are potentially suitable for use in portable instruments. The motivation for this study was to develop new concepts for portable and compact neutron detectors, for applications such as neutron dosimetry, reactor physics, and the detection of illicit nuclear material.

II. EXPERIMENTAL METHODS

Pulse shapes produced from liquid scintillators have extremely fast decay times, typically < 10 ns for electrons (gamma ray interactions) and 50-100 ns for protons (neutron scatter interactions). Consequently the use of digital PSD relies on fast waveform digitizers with ~1 ns timing resolution. Following our approach initially presented in [4], we have characterized the PSD performance of different computationally-simple digital pulse shape algorithms; (1) the 10-90% pulse rise time, (2) the pulse time over threshold, and (3) the Q-ratio (charge comparison) method. The rise time algorithm was applied to integrated pulses produced from a charge integrating preamplifier, and the later two algorithms were applied to current pulses produced directly from the PMT anode. A high-speed 500 MS/s, 8-bit digitizer captured the shape of each pulse with 2 ns time resolution. An 800 MHz Pentium P-III PC running dedicated Lab-view data acquisition soft ware was used to process the digitized waveform on an event-by-event basis. The use of the integrating preamplifier can potentially improve the signal to noise ratio of the pulses, although at the risk of degrading the fastest pulse rise time. Conversely, direct processing of the current pulses provides the simplest circuit connection and fastest pulse shapes.

Fig.1 shows a schematic illustration of the three digital PSD algorithms studied in this work. The rise time algorithm determines the time at which the light pulse reaches a certain fraction of its maximum amplitude. In this algorithm the upper and lower amplitude thresholds can be arbitrarily varied, for example from a typical 10%-90% range to an extended 5%-95% range.

* Corresponding author. Tel.: +44 (1483) 689422; fax: +44 (1483) 686781.

0-7803-8257-9/04/$20.00 © 2004 IEEE.

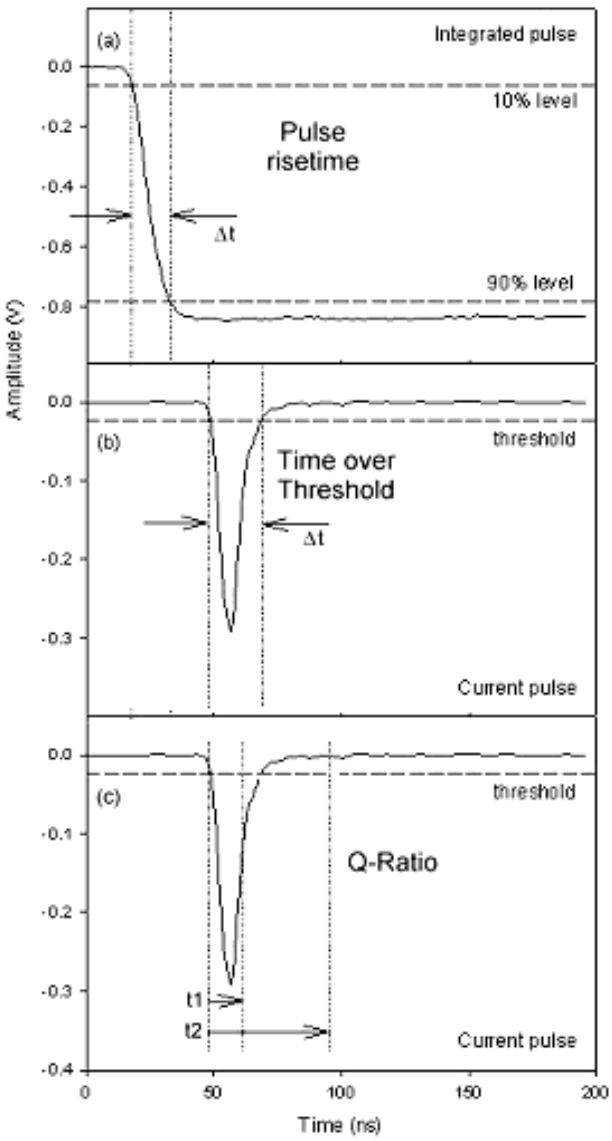

Fig. 1 Graphical representation of three different pulse shape algorithm (a) Pulse rise time (b) pulse time over threshold (c) pulse Q-ratio

The PSD algorithms that were applied to non-integrated current pulses are the 'time over threshold' and 'Q-ratio' algorithms. The time over threshold method measures the time width that the pulse remained over the threshold amplitude, typically equal to five times the 1σ noise of the pulse baseline and so provides a direct sample of the long-lived component in pulse shape. The 'Q-ratio' algorithm, which was also applied directly to current pulse, integrates the pulse into two different time gates as shown in Fig. 1(c). A short gate integrates only the charge of fast component (Q_P) while the second gate integrates the charge corresponding to the total pulse (Q_T). The PSD parameter is given by the ratio Q_T/Q_P and is sensitive to the asymmetry of the pulse shape. The effectiveness of PSD by this method depends on the position of both time gates, which have typical values of 15 ns and 70 ns.

In all cases, a digital filter and base-line correction is applied to each pulse. The filter is a five point running-average binomial filter [7] which is chosen for fast computational speed.

III. Results

The performance of the digital PSD algorithms was first investigated using BC501A unloaded liquid scintillator. The 10-90% rise time algorithm was applied to integrated pulses obtained from the preamplifier, whilst the other two algorithms i.e. time over threshold and Q-ratio algorithms were used for current pulses with no preamplifier. Saturated pulses with amplitude greater than the digitizer full-scale range were rejected.

One of the primary aims of this work is to develop fast digital algorithms that are not computationally intensive. Consequently we have investigated the PSD performance of our system using a two dimensional histogram for each of above three algorithms. For each algorithm the abscissa of the 2D histogram represents the signal amplitude, while the ordinate contains the relevant pulse PSD parameter. Fig. 2 shows two-dimensional plots of 10-90% rise time of *integrated* pulses versus amplitude from BC501A.

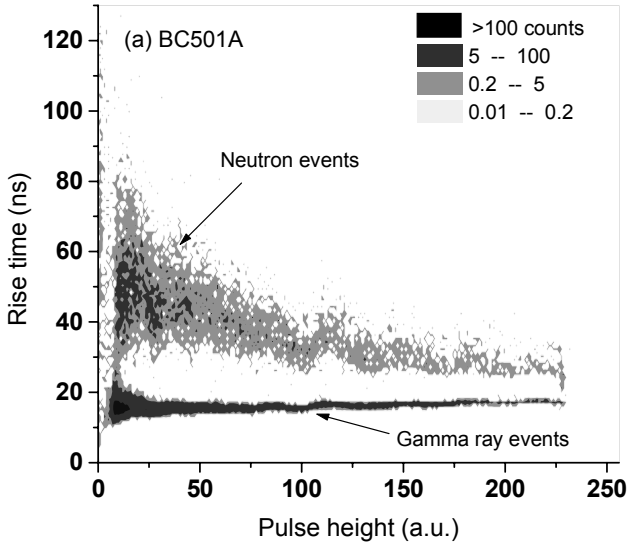

Fig. 2. Rise time versus pulse height plot at low gain setting showing n/γ PSD from BC501A

The gamma ray events lie on a well-defined narrow 'horizontal' line with a rise time of 18-20 ns, which is limited by the rise-time of the preamplifier in this case. Neutron scatter events lie on a well-separated locus, varying from ~30 ns rise time at high energy to ~60 ns rise time at low energy. There is clear n/γ discrimination between the two classes of events in BC501A. The corresponding data acquired at high gain from BC501A is shown in Fig. 3. At high gain fast neutron events are only weakly visible, as the spectra are dead-time limited by the more intense low energy gamma events.

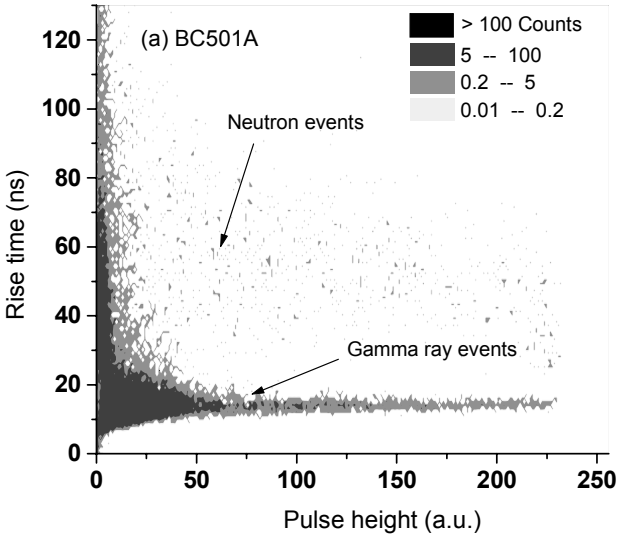

Fig. 3. Rise time versus pulse height plot at high gain setting showing n/γ PSD from BC501A.

By applying energy gates to the 2D data shown in Fig. 2 and Fig. 3, the rise time distributions at low and high energies are obtained. Using the approach of reference [2] a Figure-of-Merit (FOM) was defined as:

$$FOM = \frac{S_{n\gamma}}{F_n + F_\gamma} \qquad (1)$$

Where $S_{n\gamma}$ is the separation between the centroid of the neutron peak and the centroid of the gamma peak in the rise time spectrum, and F_n, F_γ are the full width half maximum values of the two peaks respectively. Fig. 4 shows amplitude-gated rise time spectra for BC501, projected from the two dimensional data of Fig. 2. The FOM values deduced from the low gain data are (a) 1.4 and (b) 1.5 respectively.

We also investigated the digital PSD performance of current pulses acquired from BC501A by connecting the digitizer directly to the PMT signal, terminated with a 50Ω input impedance. This measurement allowed a comparison of PSD performance between current and integrated pulses, and a check of the possible influence of the preamplifier rise time on the discrimination performance. The 'time over threshold' algorithm was used to determine the decay time of the each pulse. Fig. 5 shows the resulting two-dimensional plot of time over threshold versus pulse amplitude, also acquired at low gain.

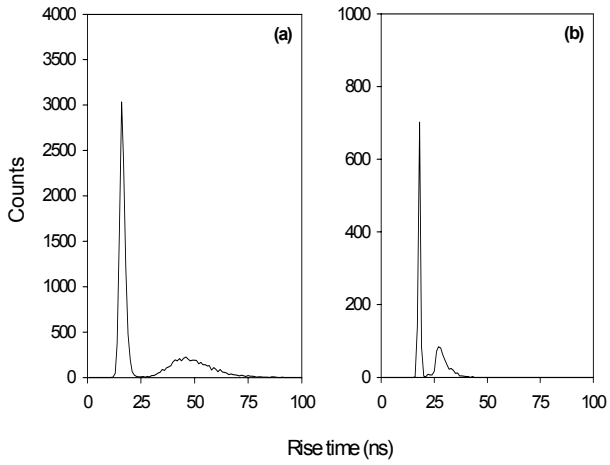

Fig .4. Rise-time spectra from BC501, projected from the data in Fig2. The PSD FOM in each case is (a) 1.4 at low energy and (b) 1.5 at high energy.

The data show good n/γ discrimination with FOM values of 0.8 and 1.4. However, at low energies the discrimination is not well defined due to overlap between the neutron and gamma ray data.

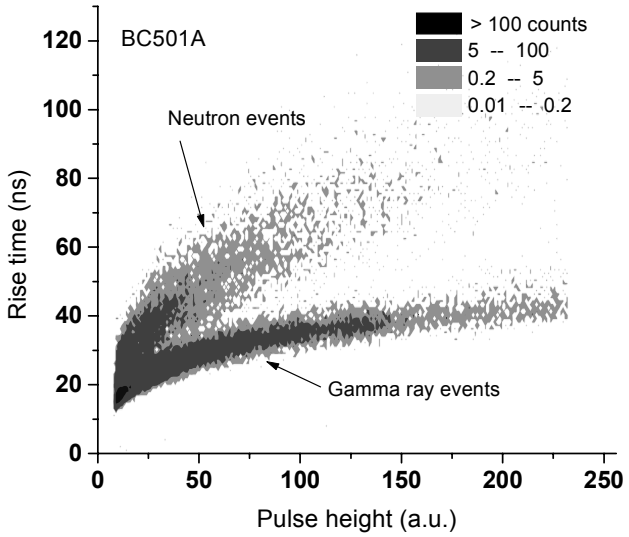

Fig. 5. 'Time over threshold' versus pulse height plot using current pulses from BC501A at low gain.

We also investigated the PSD performance of the Q-ratio algorithm, as shown in Fig. 1(c). This algorithm determines the partial and total charge by summing the amplitude of each pulse for two different time windows typically 15 ns and 70 ns respectively. On the 2D display one can observe the two well-separated components corresponding to γ-rays and neutron

events as shown in Fig. 6. The corresponding one-dimensional plot, at two different energy gates is shown in Fig. 7.

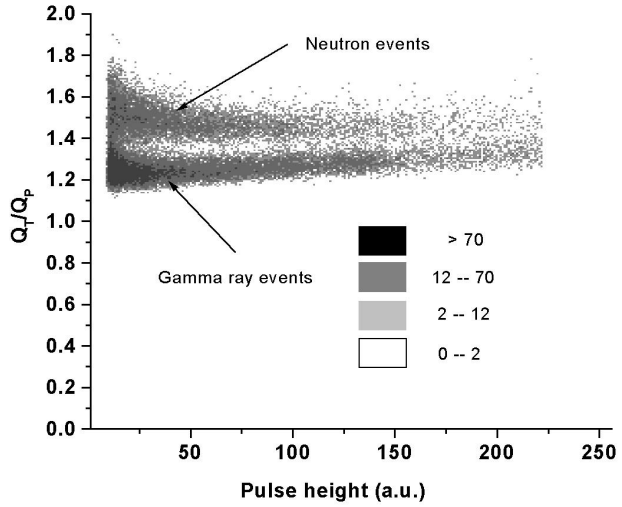

Fig. 6. The 2D spectra Q_T/Q_P versus pulse height using current pulses from BC501A showing n/γ PSD.

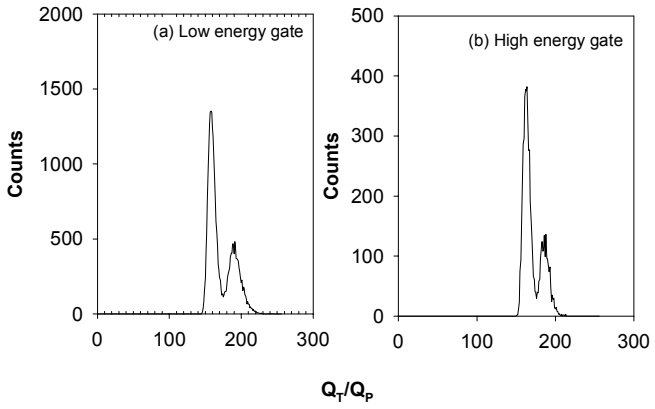

Fig. 7. The n/γ discrimination spectra, projected from the data in 6 for lower and high-energy gates. The PSD FOM in each case is 1.1

The FOM was calculated to be 1.1 for this configuration, which is independent of the pulse amplitude.

In summary, good PSD performance was observed in BC501A and BC523A using both integrated and current pulses. The FOM values achieved do not show significantly better PSD than conventional analogue techniques, but can be implemented using simple and computationally non-intensive software algorithms. Despite the relatively slow rise time of our preamplifier, rise time values calculated from integrated pulses produced good PSD performance. Similar performance was achieved by a Q-ratio algorithm applied to current pulses.

IV. Conclusion

We have investigated digital PSD techniques applied to BC501A and demonstrate the performance of relatively simple digital PSD algorithms. We applied three different digital PSD algorithms to same data set: (a) integrated pulse rise time (b) pulse time over threshold and (c) pulse Q-ratio. We use the FOM to compare the performance of these algorithms. At higher energy all the above presented methods exhibit good n/γ discrimination. At low energy, the Q-ratio method allows better separation between the neutron and gamma ray events than the time over threshold method. Consequently the Q-ratio algorithm is favorable when applied to current pulses. Present results clearly show the power of a digital system in achieving good PSD. As the performance of high-speed waveform digitizers continues to improve, such digital pulse processing techniques are well suited for use in portable neutron monitors.

V. References

[1] H. Klein and S. Neumann, Nucl. Instr. and Meth. A **476,** (2002) 132-142.

[2] G. Ranucci, Nucl. Instr. Methods, Vol. A354, (1995) 389-399.

[3] J.H. Heltsley, L. Brandon, A. Galonsky, L. Heilbraun,, B.A. Remington, S. Langer, A. Vander and J. Yourkon, Nucl. Instr. and Meth. **A263** (1988) 441.

[4] S. D. Jastaniah and P. J. Sellin, IEEE Trans. Nucl. Sci. 49, (2002) 1824-1828

[5] N. V. Kornilov, V. A. Khriatchkov, M. Dunaev, A. B. Kagalenko, N. N. Semenova, V. G. Demenkov, and A. J. Plompen, Nucl. Instr. and Meth. A **497,** (2003) 467-478.

[6] S. Marrone, D. Cano-Ott, N. Colonna, C. Domingo, F. Gramegna, E. M. Gonzalez, F. Gunsing, M. Heil, F. Kappeler, and P. F. Mastinu, Nucl. Instr. and Meth. A **490,** (2002) 299-307.

[7] P. Marchand and L. Marmet, Review of Scientific Instruments **54,** (1989) 1034-1041.

[8] S. C. Wang, C. C. Hsu, R. W. S. Leung, S. L. Wang, C. Y. Chang, C. P. Chen, K. C. Cheng, T. I. Ho, W. P. Lai, and H. M. Liu, Nucl. Instr. and Meth. A **432,** (1999) 111-121.